Elliptical experimental detonation

Romane BABIN, Ashwin CHINNAYYA, Vincent RODRIGUEZ
Institut Pprime, UPR 3346 CNRS, ENSMA, University of Poitiers
BP 40109, 86961 Futuroscope-Chasseneuil, France

1 Introduction

Gaseous detonation is a supersonic reactive wave, dynamics of which is mainly affected by the shock curvature [1] and its unsteadiness [2, 3]. In the case of a steady detonation, several physical mechanisms such as wall boundary layer growth, lateral product expansion (see [4] for the common flow description of these two canonical configurations) among others, will curve the mean leading shock and induce detonation velocity deficits and may cause extinction. Radulescu et al. [5] have related the shock curvature to that of particular channel, drawing of which followed that of an exponential horn. On the contrary of these divergent flows, the detonation wave can develop a Mach stem when the shock wave bends over a concave surface [6, 7]. In practical applications such as in an annular channel rotating detonation engine, two radius of curvature are present: one is related to the curvature of the combustion chamber [8], and the second is due to the product expansion [9, 10]. Xiao et al. [11] have also recently analyzed their experimental in a narrow exponential horn with two radius of curvature: one related to the geometric channel expansion, the other related to the boundary layer growth.

These two latter examples call attention to the possible combined effects of each of the two curvatures of the shock surface, and to a lesser extent to the confinement curvatures, even if they should not be confused. The detonation propagation in a tube is well-documented [12]. In the case of an elliptical tube, two generic curvatures are present. Lui et al. [13] reported results on detonation transmission through orifices of different shapes. The present study reports some experimental results on detonation propagation in an elliptical cross-section tube, with mixtures of increasing irregularity: $2H_2+O_2+N_2$, $2H_2+O_2$ and CH_4+2O_2, for initial pressures ranging from 12 kPa to 100 kPa. Section 2 presents the experimental set-up and methodology, and section 3 presents the soot-foil recordings obtained for one ratio of the axis lengths (r=½) and the associated discussions.

2 Experimental set-up and methodology

The experimental set-up is a detonation tube that consists of two main parts, namely the circular cross-section tube and the elliptical cross-section inserted inside the latter at its end. The latter was designed with the help of a 3-D printer. The aim was to generate a detonation wave at one end of the circular cross-section tube that propagated steadily before entering the elliptic section, in which the detonation then readjusted itself to the new geometry, according to the initial pressure. The circular detonation tube is 4-m long and its cross-section inner diameter is 52-mm. The elliptic section is 0.5-m long, and

Correspondence to: vincent.rodriguez@ensma.fr

the major axis and the minor axis are 50-mm and 25-mm long, respectively. The ration r of the axis lengths is then equal to ½. Figure 1 shows a schematic of the experimental set-up.

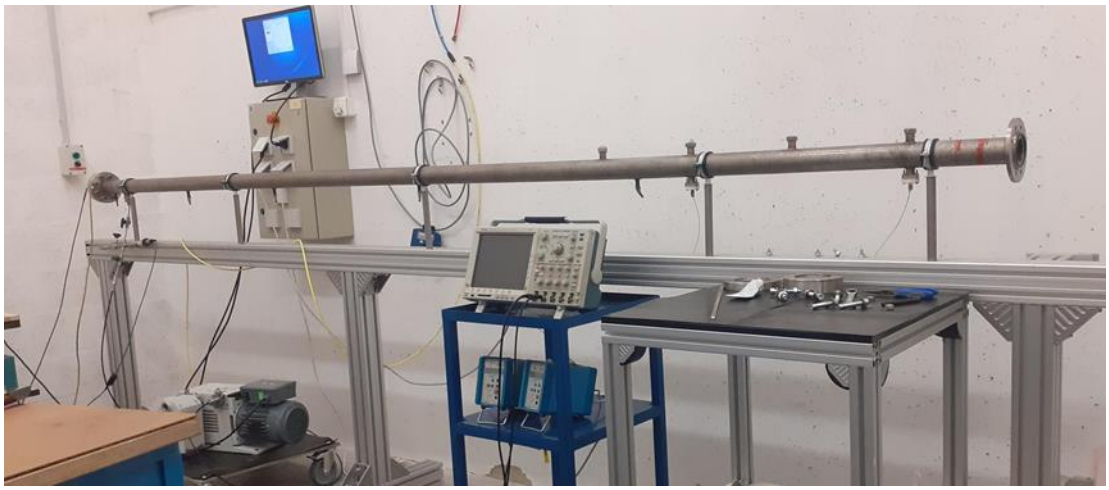

Figure 1: Schematics of the experimental set-up.

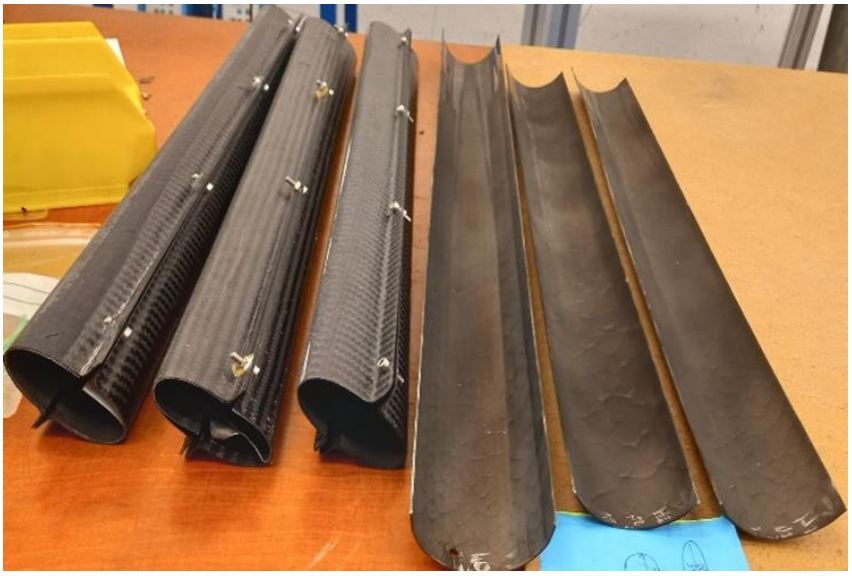

Figure 2: Elliptical cross-section tubes (left) coated with aluminum so that to deposit soot for detonation cell recordings. Semi-circular soot-foil (right) to characterize the detonation in the circular cross-section tube before entering the elliptic section.

Two series of experiments varying the initial pressure p_0 were done for each mixture: one for the reference states without the elliptic section, and a second one with the elliptic section inserted inside the circular tube at its end. Soot-covered semi-circular foils (Fig. 2) positioned at the end of the tube were used to record the structure of the detonation cells for the reference circular state. The elliptic section can be opened into two parts to allow deposit of carbon soot, in order to observe the cellular detonation structures. The detonation in the tube resulted from the deflagration generated by the spark of an automotive plug, and transition to detonation was then obtained by a 1-m long Shchelkin spiral positioned immediately ahead of the plug. The set-up was vacuumed before injecting the premixed

composition prepared in a separate tank using the partial-pressure method. Two Kistler 603B pressure transducer (1μs response time, 300 kHz natural frequency, each coupled with a Kistler 5018A electrostatic charge amplifier with 200 kHz band width) were used to check that the CJ detonation regime was achieved before entering the elliptic section. The reactive gases were the stoichiometric mixtures $2H_2+O_2+N_2$, $2H_2+O_2$ and CH_4+2O_2, for initial pressures ranging from 12 kPa to 100 kPa initially at $T_0 \sim 294$ K. There are characterized from regular ($2H_2+O_2+N_2$) to irregular (CH_4+2O_2) according the usual characterization of detonation-cell regularity.

3 Results

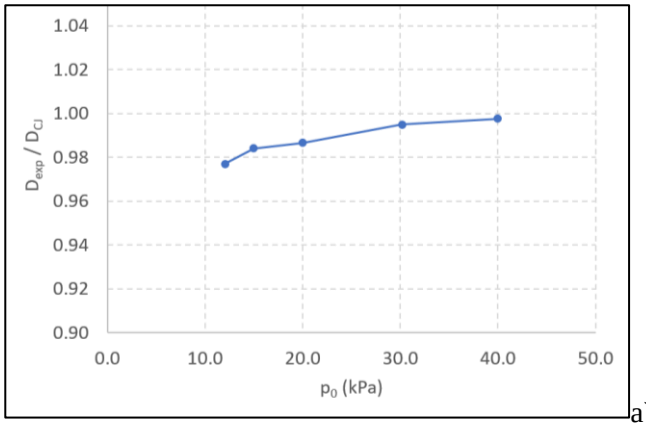

a)

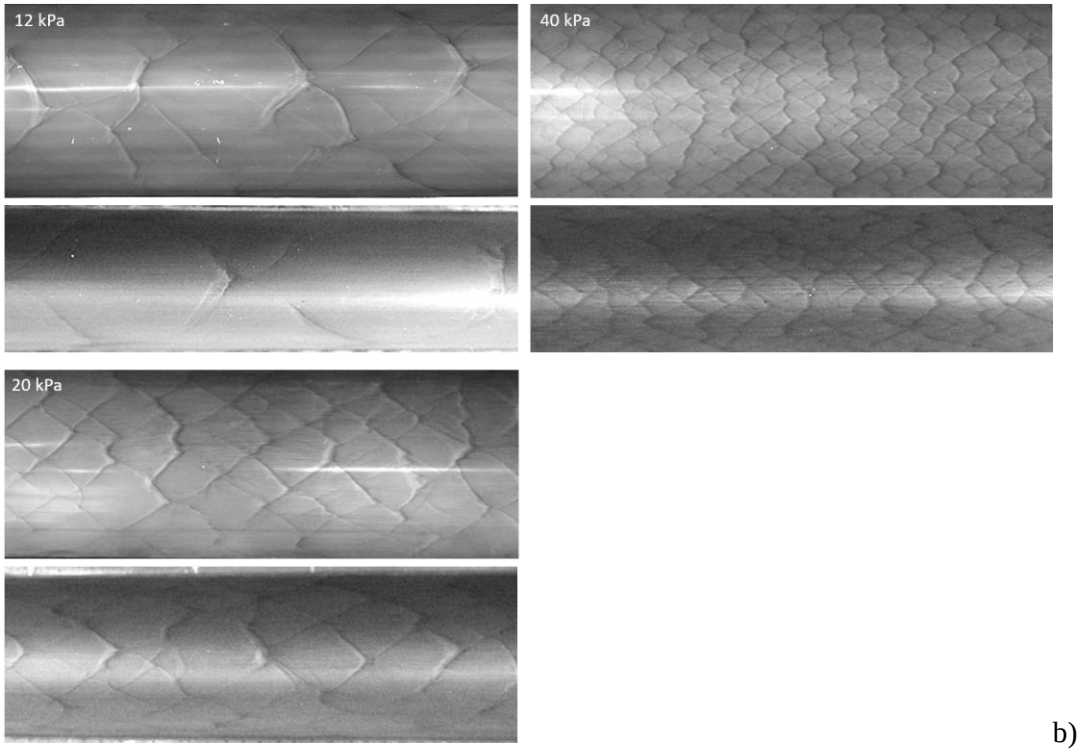

b)

Figure 3: a) Detonation deficit for $2H_2+O_2+N_2$ as a function of the initial pressure in circular tube. b) Cellular recordings for different pressures for circular (top) and elliptical (bottom) tubes.

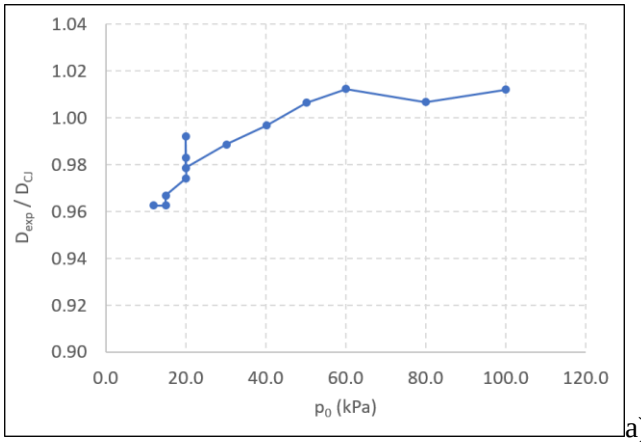

a)

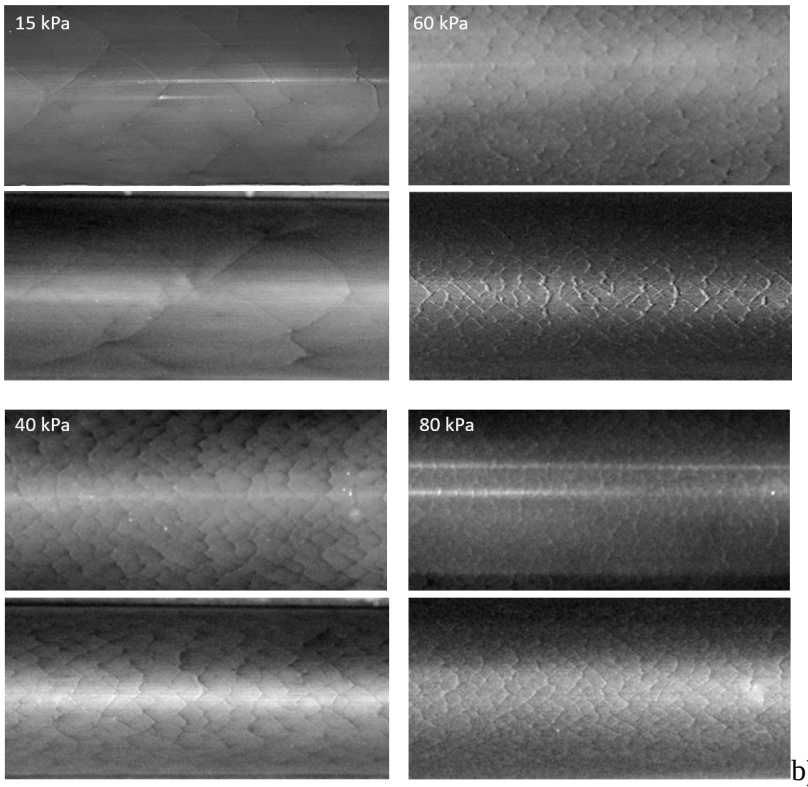

b)

Figure 4: a) Detonation deficit for $2H_2+O_2$ as a function of the initial pressure in circular tube. b) Cellular recordings for different pressures for circular (top) and elliptical (bottom) tubes.

Figures 3, 4 and 5 present the non-dimensionalized experimental detonation velocity by theoretical CJ detonation velocity (D_{exp}/D_{CJ}) as a function of the initial pressure p_0 for the mixtures $2H_2+O_2+N_2$, $2H_2+O_2$ and CH_4+2O_2, respectively. They also show the soot-foil recordings for circular cross-section (top images) and the elliptic cross-section (bottom images) for initial pressures ranging from 12 kPa to 100 kPa.

The first main observation is that the ratio D_{exp}/D_{CJ} decreases with the decrease of p_0. Moreover, the detonation velocity decrease is smoother with the mixture regularity. As the detonation velocity deficit increases, the cell size increases. This can be clearly seen for $2H_2+O_2+2N_2$ between 12 and 20 kPa, for $2H_2+O_2$ between 15 and 40 kPa and for CH_4+2O_2 between 12 and 50 kPa. Secondly, the cellular patterns show that the detonation-cell mean width is larger for the elliptic cross-section than the circular cross-

section, for the same initial pressure p_0. Moreover, the head and tail of the cell have a clear tendency to be locked at the vertices of the ellipsis, as the pressure decreases and losses become prominent.

The stoichiometric methane mixture has shown some specific features (see Fig. 5). In the circular tube, a classical substructure is present near the apex of the cell (see Fig. 5 at 12 kPa). It is still present to a lesser extent in the elliptical section. At 12 kPa, between 1 and ½ cell detonation can be seen in the circular case. What was more remarkable was the presence of repeating sequence of extinctions and re-ignitions of detonation that can be inferred from the absence and presence of cells at 12 kPa in the elliptical case.

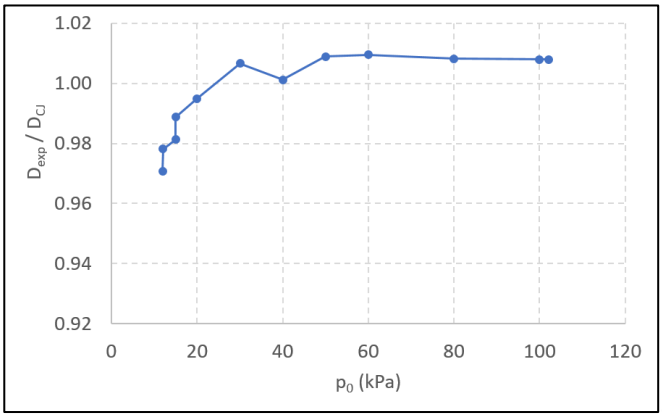

a)

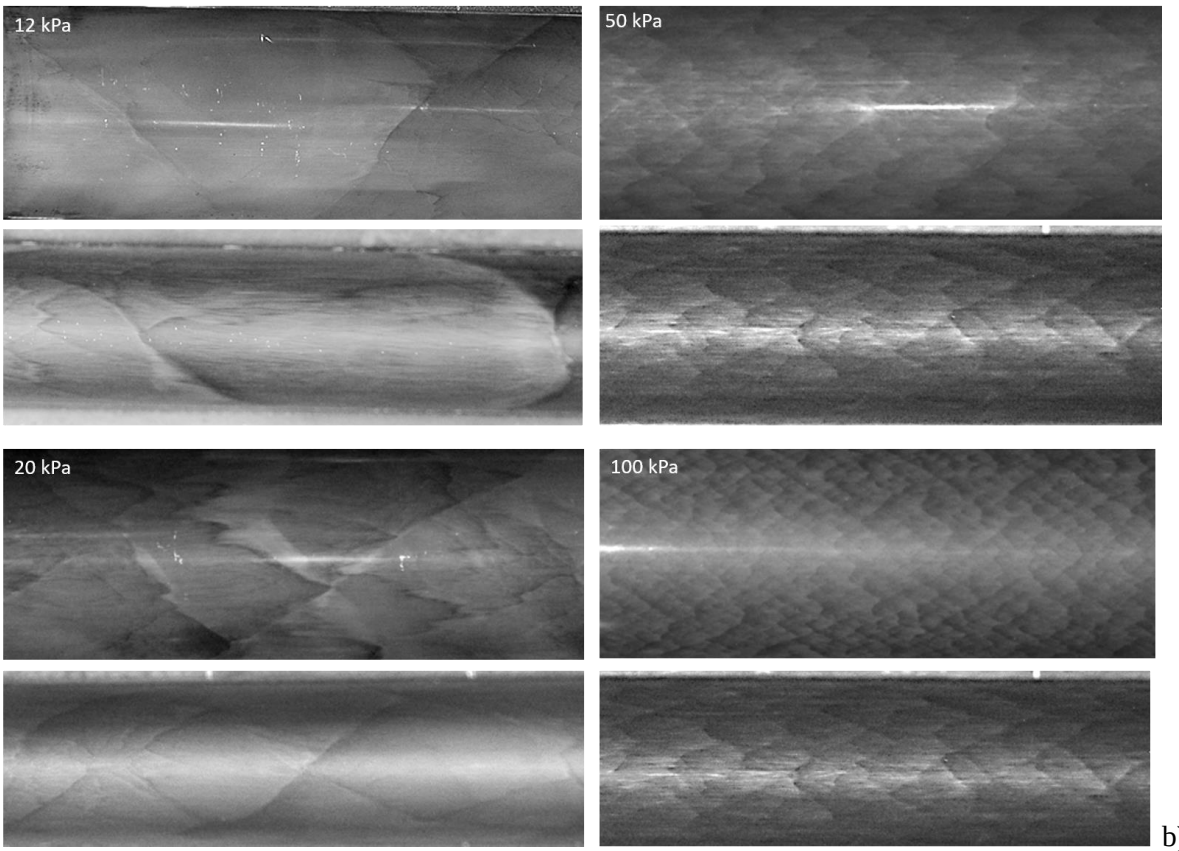

b)

Figure 5: a) Detonation deficit for CH_4+2O_2 as a function of the initial pressure in circular tube. b) Cellular recordings for different pressures for circular (top) and elliptical (bottom) tubes.

4 Discussions

Experimental results of detonation propagation in circular and elliptical tubes have been performed, for three different mixtures, of increasing regularity. The ratio of the minor and major axis was one half. Detonation velocity deficits in the circular case have been obtained, as the initial pressure was decreased. The cells were larger in the ellipsis. Even if the detonation velocity could not be measured due to experimental limitations, we can infer that the reduced radius in the minor axis played a key role in enhancing the losses. The cells seemed to be locked in this axis. In the more unstable case, the presence of a repeating sequence of extinctions and re-ignitions of detonation has also been observed in the elliptical case, mechanism of which is not yet elucidated. It is hoped that speed measurements will be provided for the elliptical cases as well characterized propagation limits

There is a need for more results with different ratios of the axis lengths, and relate the different phenomena to the velocity deficits, with a possible effective mean radius.

Acknowledgements

This work was supported by the CPER FEDER Project of *Région Nouvelle Aquitaine* and pertains to the French government program *"Investissements d'Avenir"* (EUR INTREE, reference ANR-18-EURE-0010). Part of this research was supported by the French National Research Agency (ANR) under the project ANR-21-CE05-0002-01.

References

[1] Lee, JHS. (1984). Dynamic parameters of gaseous detonations. Annu. Rev. Fluid Mech. 16.1:311-336.

[2] Shepherd JE. (2009). Detonation in gases. Proc. Combust. Inst. 32.1: 83-98.

[3] Radulescu MI (2020). On the shock change equations. Phys. Fluids 32.5: 056106.

[4] Chinnayya A, Hadjadj A., Ngomo D. (2013). Computational study of detonation wave propagation in narrow channels. Phys. Fluids 25.3:036101.

[5] Radulescu MI, Borzou B. (2018). Dynamics of detonations with a constant mean flow divergence. J. Fluid Mech. 845:346-377.

[6] Ben-Dor G. (2007). Shock wave reflection phenomena. Vol. 2. New York: Springer.

[7] Rodriguez V., Jourdain C., Vidal P., Zitoun, R. (2019). An experimental evidence of steadily-rotating overdriven detonation. Combust. Flame 202:132-142.

[8] Kawasaki A., Inakawa T., Kasahara J., Goto K., Matsuoka K., Matsuo A., Funaki I. (2019). Critical condition of inner cylinder radius for sustaining rotating detonation waves in rotating detonation engine thruster. Proc. Combust. Inst. 37(3):3461-3469.

[9] Anand, Vijay, and Ephraim Gutmark. "Rotating detonation combustors and their similarities to rocket instabilities." Progress in Energy and Combustion Science 73 (2019): 182-234.

[10] Reynaud M., Taileb S., Chinnayya A. (2020) Computation of the mean hydrodynamic structure of gaseous detonations with losses. Shock Waves 30.6:645-669.

[11] Xiao Q., Sow A., Maxwell BM., Radulescu MI. (2021). Effect of boundary layer losses on 2D detonation cellular structures. Proc. Combust. Inst. 38(3) :3641-3649.

[12] Lee JHS. (2008). The detonation phenomenon. Cambridge University Press.

[13] Liu YK, Lee JHS, Knystautas R. (1984). Effect of geometry on the transmission of detonation through an orifice. Combust. Flame 56(2):215-225.